



HAL
open science

Going beyond the reflectance limit of cholesteric liquid crystals

Michel Mitov, Nathalie Dessaud

► **To cite this version:**

Michel Mitov, Nathalie Dessaud. Going beyond the reflectance limit of cholesteric liquid crystals. Nature Materials, 2006, 5 (5), pp.361-364. 10.1038/nmat1619 . hal-03588685

HAL Id: hal-03588685

<https://hal.science/hal-03588685>

Submitted on 11 Mar 2022

HAL is a multi-disciplinary open access archive for the deposit and dissemination of scientific research documents, whether they are published or not. The documents may come from teaching and research institutions in France or abroad, or from public or private research centers.

L'archive ouverte pluridisciplinaire **HAL**, est destinée au dépôt et à la diffusion de documents scientifiques de niveau recherche, publiés ou non, émanant des établissements d'enseignement et de recherche français ou étrangers, des laboratoires publics ou privés.

Going beyond the reflectance limit of cholesteric liquid crystals

Michel Mitov* and Nathalie Dessaud

Centre d'Elaboration de Matériaux et d'Etudes Structurales, CEMES, CNRS,

BP 94347, 29 rue Jeanne-Marvig, F-31055 Toulouse cedex 4, France

*email: mitov@cemes.fr

Cholesteric liquid-crystalline states of matter are widely present in nature: atherosclerosis¹, arthropods cuticles^{2, 3}, condensed phases of DNA⁴, plant cell walls^{2, 5}, human compact bone osteon⁶, chiral biopolymers⁷⁻¹⁰. The self-organized helical structure produces unique optical properties¹¹. Light is reflected when the wavelength matches the pitch (twice periodicity); cholesteric liquid crystals are not only coloured filters but also reflectors and polarizers. But, by the theory, the reflectance is limited to 50% of ambient (unpolarized) light because circularly polarized light of the same handedness than the helix is reflected. Here we elaborate a cholesteric medium for which the reflectance limit is exceeded. Photopolymerizable monomers are introduced in the volume of a cholesteric exhibiting a thermally-induced helicity inversion and the blend is then UV-cured when the helix is right-handed. Due to memory effects brought by the polymer network, the reflectance exceeds 50% when measured at the temperature assigned at a cholesteric helix with the same pitch but a left-handed sense before reaction. Since cholesterics are used as tunable bandpass filters, reflectors or polarizers and temperature or pressure sensors¹², novel opportunities to modulate the reflection over the whole light flux range, instead of only 50%, are offered.

The use of light spectrum colours is important in information technologies, and colour information is provided by nature – plants, butterflies, birds, beetles – via petals, wings or bodies due to structural variations¹³. The exocuticles of many beetles have remarkable optical properties, such as selective reflection of left circularly polarized light, high optical rotation of transmitted light, and a brilliant metallic appearance¹⁴⁻¹⁶. They behave as optical analogues of cholesteric liquid crystals (CLC): these properties originate from a twisted arrangement of chitin biomolecules. Light is selectively reflected from a CLC when the wavelength λ_0 matches the pitch p of the helix such that $\lambda_0 = n p \cos\theta$, where n is the effective refractive index (average of ordinary and extraordinary indices) and θ is the angle between the light propagation direction and the helix axis; outside the reflection band, a CLC affects neither the amplitude nor the state of polarization of the incident light. The reflected light is circularly polarized with the same handedness as the helix, which means that 50% of unpolarized incident light is reflected at the very best¹⁷. However, an exception was found: for *Plusiotis Resplendens*, the reflected light consisted of both left circular and right circular polarization¹⁶. This gold beetle has perfected the optical trick of using a $\lambda/2$ plate that functions as a half wave plate for the wavelengths between 520 and 640 nm. Indeed, by placing two similar filters either side a $\lambda/2$ plate, the right-handed polarized light that is passed through the first filter is converted into left-handed polarized light by the $\lambda/2$ plate and reflected from the second filter. In this way a simple notch filter is produced.

Without analogy in nature nor technology, we elaborated a single-layer of LC gel whose optical characteristics go beyond the 50% reflectance limit. We used CLCs exhibiting the phenomenon of helicity inversion. Helix inversion occurs when the handedness of the helical structure is changed with temperature, leading to a nematic state (infinite-pitch CLC) at the inversion temperature^{18,19}. Due to the temperature-sensitivity of the chirality, helix inversion compounds are excellent systems to probe the microscopic origin of the chirality in LC phases. Two general explanations for the helix inversion behaviour have been suggested. In one, the statistical distribution of the many molecular conformations shifts with changing the temperature^{20,21}. In the other, the competition between the different temperature dependences and opposite chiralities of multiple chiral centers causes the helix inversion^{22, 23}. Experimental support for the first explanation comes from nematic systems with chiral dopants^{24, 25}, whereas results verifying the second explanation use diastereomeric LC compounds^{26, 27}. We have carried out optical measurements in the cholesteric phase of a LC blend introduced into a 50 ± 10 μm thick glass sandwich-cell (see Methods for the blend and cell characteristics). The phases were identified using polarizing microscopy. The cholesteric to isotropic phase transition occurred at 114°C . The sample showed a helicity inversion at $T_c = 92^\circ\text{C}$ and exhibited a planar nematic texture with four extinction positions between crossed polarizers. The transmittance spectra were investigated by IR spectroscopy between 2.50 and 4.50 μm (see Methods for the spectroscopy details). Below T_c , the helix is left-handed and the reflection wavelength changes inside the investigated range from 2.8 to 4.2 μm when the temperature increases; above T_c , the helix is right-handed and the wavelength changes from 4.4 to 3.8 μm inside the investigated range.

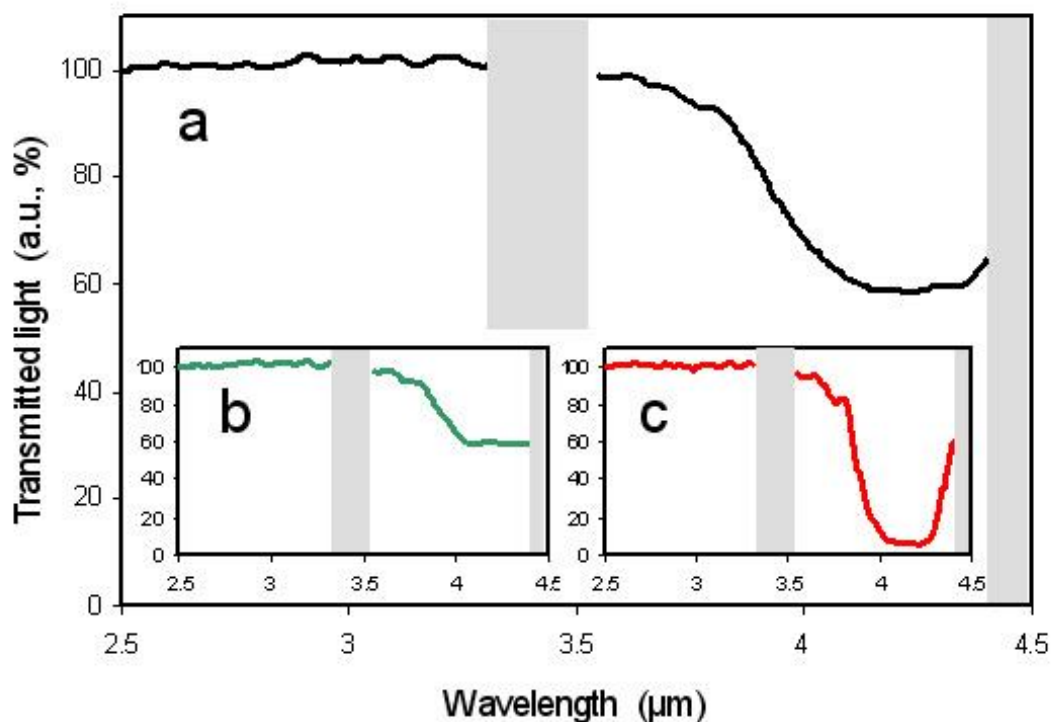


Figure 1. Transmission spectra. Normalized transmission spectra at 112°C before UV-reaction, when the incident light is unpolarized (a) or after the introduction in the light beam path of a left (b) or right (c) circular polarizer. Due to the polarization selectivity rule and the fact that the helix is here right-handed, the light flux is close to 40% when the incident light is unpolarized or left circularly polarized, and close to 90% when the incident light is right circularly polarized. See the Methods section for the normalization conditions and the Supplementary information details on the nature of polarizers. The shadowed areas mark the chemical absorption bands.

Figure 1 shows the transmittance spectra of the cell for different polarization cases of incident light at 112°C, when the reflection wavelength is equal to 4.2 μm. Left- and right-circular polarizers were fabricated with a two-compound (enantiomers) CLC mixture; here the polarizers are thus also reflectors (see Supplementary information on the nature of polarizers). The cell exhibits a very well aligned reflective (planar) texture,

due to a confinement ratio (thickness : pitch ratio) equal to 18 ± 6 , fitting for clear-cut reflection peaks. Due to the fact that the helix is right-handed, the maximum reflection intensity is close to 40% – at least less than 50% – when the incident light beam is unpolarized (**Fig. 1.a**), or after the introduction of a left-circular polarizer (**Fig. 1.b**), and it is close to 90% after the introduction of a right-circular polarizer (**Fig. 1.c**). Classical behaviours are thus checked. Then, the cell is cured with UV-light (with the wavelength of maximum intensity of 0.1 mW/cm^2 centred on 365 nm) at 112°C for 4 hours, while the cholesteric helix is right-handed. When the reflectance properties are investigated at 112°C , the reflection wavelength is shifted from 4.2 to 3.8 μm as a result of polymer network formation in the LC matrix. The helical pitch of the blend is believed to slightly decrease in relation with the volume shrinkage coming from the reaction of polymerization and crosslinking. Such a behaviour had previously been observed during the formation of three-dimensionally ordered polymer networks with a helical structure²⁸.

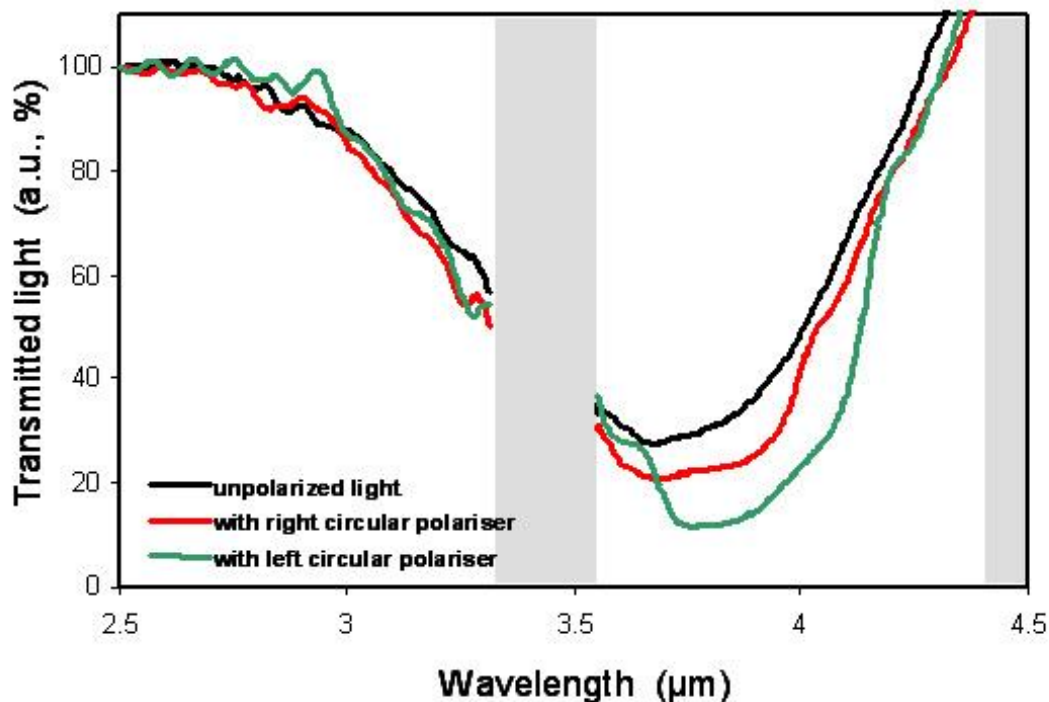


Figure 2. Transmission spectra. Normalized transmission spectra at 60°C, after UV-reaction at 112°C, when the incident light is unpolarized (a) or a left (b) or a right (c) circular polarizer is introduced in the light beam path. Whatever the polarization of the incident light is, the reflectance of cholesteric film goes over the limit of 50%. A chemical absorption band approaches close to 4.5 μm , as a result of which the normalized transmitted intensity diverges above 100%. The shadowed areas mark the chemical absorption bands.

Figure 2 shows the transmission spectra of the same cell, after cooling, at a temperature equal to 60°C for which, before gelation, the selective reflection is close to 3.8 μm by being associated to a left-handed helix. From **Figure 2**, using unpolarized light or introducing a right or left circular polarizer in the beam path, we deduce that the reflected intensities are respectively equal to 72, 78 and 88%. These quantities are

reduced to the flux of the unpolarized light source at $2.5\ \mu\text{m}$ (see Methods for the normalization conditions). Now, we can also consider as the reference flux the light being incident on the cell – *ie* after having crossed a circular polarizer (reflecting 50% of the source); therefore we deduce that the reflected intensities are equal to: 76% (*ie*: $(88 - 50) \times 2$) of a left circularly polarized incident light and to 56% (*ie*: $(78 - 50) \times 2$) of a right one. In conclusion, whatever the polarization of the incident light is, the reflectance of the cholesteric film goes over the reflectance limit of 50%.

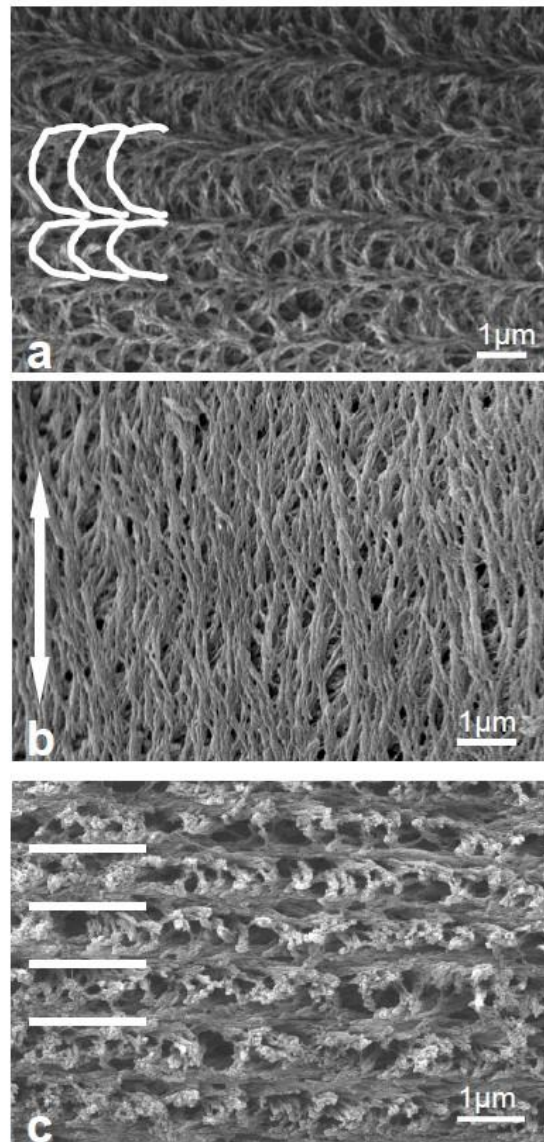


Figure 3. SEM images of the polymer network formed in the cholesteric phase.

The helical structure has been transferred onto the polymer morphology. The polymer fibrils draw stacked rows of parallel arcs which appear when the cut direction is oblique to the helical axis (**a**); these arcs are enhanced in white on the left part of the picture. The fibres are viewed as parallel together in a cut direction parallel to the surfaces (**b**); the double-headed arrow represents the mean orientation of the fibres: this micrograph shows the locally transferred nematic order. A layered system of fibres appears when the polymer network is cut and viewed in a direction strictly perpendicular to the surfaces (**c**); white bars indicate the position of a few layers. See the Methods section for details on material preparation and observation conditions. The scale bar on each image represents 1 μm .

The polymer morphology, as investigated by scanning electron microscopy (SEM), exhibits smooth polymer strands (**Fig. 3**), like the signature of a good solubility of the monomers within the LC; the behaviour may be understood in the context of the Flory-Huggins model of polymer solubility²⁹, which is the primary factor determining the network morphology. **Figure 3.a** displays polymer fibrils as stacked rows of parallel arcs which appear when the cut direction is oblique to the helical axis. Such arced patterns were visible in thin sections of biological materials: crustacean integuments³⁰, dermal plates of fishes³¹, insect cuticles^{2,3,30}, collagenous matrices of bone tissue⁶, plant cell walls⁵ and chromatin organizations for DNA⁴; they have also been observed in man-made polymer-stabilized CLCs³². The arced patterns found in these widely differing systems have a common physical origin: a twisted plywood model to account for such an architecture was proposed by Bouligand³⁰. Here, and by analogy, the architecture is as follows. The material appears to be made of superimposed lamellae of

polymer fibres, which are parallel to the glass plate (**Fig. 3.b**). We define the plane of this latter as being horizontal. Each lamella contains parallel arcs when observed in oblique sections (**Fig. 3.a**). In contrast, in vertical section – *ie*: normal to the glass plate – the arcs disappear but the stratification persists (**Fig. 3.c**). As the plane of the section approaches the plane of the layers, the arcs appear larger.

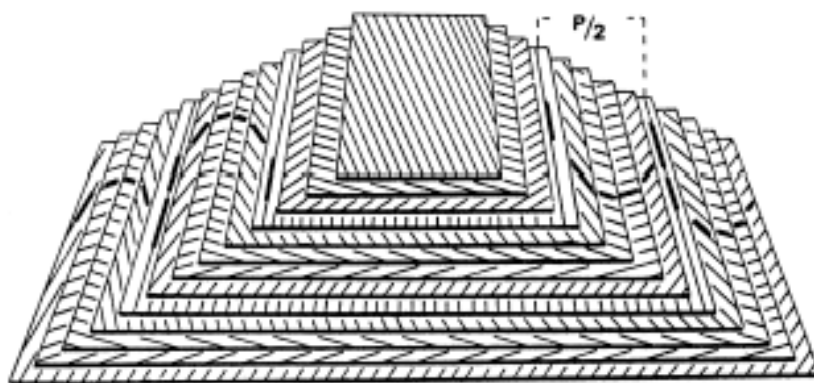


Figure 4. Three-dimensional model of the cholesteric organization. Superimposed cards represent equidistant and parallel planes. On each card the polymer fibrils are represented as parallel lines, their direction rotating by a small and constant angle from one plane to the other. A 180° rotation of the fibrils direction defines the half helical pitch. A superimposed series of nested arcs (see Fig. 3.a for analogy) is visible on the oblique side of the model. Reprinted from Ref. 36, copyright (1995) with permission from Elsevier.

In summary, and as sketched in **Figure 4**, the present system is made of polymer fibrils that are horizontal, parallel within any given horizontal plane, and with a direction that rotates continuously as one proceeds through successive levels of the bulk polymer. This is exactly the geometry of the cholesteric structure. These SEM investigations give undoubtedly evidence for the transfer of the organization of the mesophase onto the

structure of the network; the standing first result of forming a polymer network into the LC solvent is the transfer of the mesophase characteristics to the polymer network during the *in situ* polymerization³⁴. However, it is not possible from these pictures to give quantitative information about the size of the pores in which the LC component of the gel was located. Indeed, when the LC is extracted (see Methods — SEM investigations section), the polymer network collapses to some extent in the direction perpendicular to the substrates, like it was described in previous studies on polymer-stabilized LCs³⁴, and, furthermore, there is some residual LC around the network fibrils.

The gel property consisting in exceeding the reflectance limit is attributed to the cholesteric LC being divided into two distinct environments: bulk-like material and strongly network-dominated regions³⁵; LC molecules are also incorporated within the polymer strands but areas with helical states which participate to the reflection cannot be expected on such scales smaller than the pitch or even comparable to it. For the regions the furthest from the polymer strands the enclosed LC behaves bulk-like at 60°C, leading to cholesteric structures with a left-handed sense, assigned to the temperature measurement. At the closest neighbouring of polymer strands, LC material is strongly dominated by elastic interactions with the polymer network, which templates the cholesteric order when the polymerization occurs at 112°C, it means when the helix sense was right-handed. The association of both behaviours within one and only single-layer material has led to a cholesteric structure which unusually reflects more than the conventional limit of 50% of unpolarized incident light. The key function of the surface networks is to provide a thermally-stable internal memory of helicity sense; as a significant advantage in producing ordered polymer structures, the templating effect –

and consequent micro-patterning of the polymer – is achieved without external agents. On the respective localization of regions with a bulk-like or network-dominated behaviour: a distribution of imbricated regions has to be emphasized, to whom a gradient of polymer network from the top to the bottom of the cell – due to a UV-polymerization gradient – may be associated. Indeed, in the same film, one side can be dominated by a dense network with frozen in chiral order and the other area by a sparse network that does not affect much the intrinsic cholesteric LC ordering. Further investigations of polymer morphology by transmission electron microscopy will help to progress about the finer structure.

The subsequent investigation of the transmission properties of the gel with temperature is in agreement with the evolution of the Bragg reflection assigned to the free and bound fractions of LC molecules. Indeed, after curing at 112°C, the reflection evolves during a temperature decrease as follows: a peak present at 112°C is kept – and corresponds to the thermally-stable reflection due to the bound fraction – whereas a supplementary peak appears, which the position changes by closely following the thermally-induced variation of the selective reflection. This second peak comes from the free fraction of LC molecules. When a temperature equal to 60°C is reached, one single peak is recovered and the reflectance limit is exceeded (Figure 2).

In conclusion, cholesteric gels consisting of a polymer network with a helical structure containing two populations of low molar mass LC molecules which are not chemically attached to the network were produced. Each population was characterized by a band of circularly polarized light which is selectively reflected. We have described the reflection properties in the infrared region — of paramount importance for the

regulation of temperature, telecommunications or stealth applications; however, the self-assembling organic materials may be useful for a variety of photonic-bandgap applications, particularly as the phenomenon is not dependent on the choice of the position for the reflection band in the spectrum. To modulate the reflection over the whole light flux range, instead of only 50%, could lead to the realization of CLC films with exceptionally large fluxes of reflected light for smart windows in buildings and vehicles, greenhouses and other applications in which light management is desired. These are electro-optical glazing structures – made with a cholesteric film sandwiched between glass panels – with reflective and transparent modes of operation that are electrically-switchable to dynamically control electromagnetic radiation. We can also imagine reflective (polarizer-free) displays, more brilliant and with a larger scale of reflectivity levels.

Methods

LC blend. The LC blend consists of the nematic LC BL006 (from Merck Ltd.; used at 71.2 wt.%), the RM257 bifunctional photoreactive nematic compound (diacrylate from Merck Ltd.; used at 3.8 wt.%) and the chiral dopant DL6 to induce the helicity inversion (propanediol derivative, used here at 25 wt.%; for synthesis details see reference 36). The blend is introduced by capillarity at 90°C into the experimental cell. The helicity sense of the blend as a function of temperature is determined as follows. We used a series of CLC polarizers which the pass-band is tuned with the reflection wavelength of the blend at each temperature of the investigation (see the Supplementary information about the nature of polarizers). For the determination of the helicity sense of the cholesteric sample, we put a given circular polarizer between the light beam and the

investigation cell. As an example, if the polarizer is right circular, the light transmitted through the cell is then close to 100 (0) % of the light transmitted by the polarizer if the helicity sense of the cell is left (right). See reference 17 for more details about the admitted convention for the cholesteric helicity sense in relation with the type of circularly polarized light.

Experimental cells. We used 50 ± 10 μm thick indium tin oxide (ITO)-coated glass sandwich-cells (from EHC Co. Ltd) with a planar alignment due to polyimide layers which were uniaxially rubbed and assembled at an 180°C angle with respect to each rubbing direction.

IR spectroscopy. Transmittance spectra were investigated by using a Perkin Elmer IR spectrophotometer, coupled with a Mettler hot stage, with a compartment in which different narrow band circular polarizers can be positioned. When measurements under polarized-light conditions were required, the baseline was recorded with the introduction in the light beam of the cell placed at the helix inversion temperature $T_c = 92^\circ\text{C}$ with, in the same time, a cell filled with 100% of BL094 (BL094 is one of the two enantiomers which are mixed to fabricate the polarizers and to tune the pass-band position and the polarization sense). These baseline conditions allow to concentrate the investigation on the Bragg reflection phenomenon: the cell at T_c was there to remove from the transmitted signal the signature of the chemical bonds absorption and losses in diffusion associated to the experimental cell whereas the cell filled with BL094 was there to remove from the transmitted signal the signature of the chemical bonds absorption present in the polarizer (fabricated with a blend of BL094-BL095

enantiomers). For consistency reasons, we kept the same baseline conditions (*ie*: even with the presence of the cell filled with BL094) when the investigations under unpolarized light were done. All spectra were normalized to have an amount of light transmitted of 100% at 2.5 μ m, *ie* for a wavelength far from the reflection band. On the spectra, the shadowed areas mark the chemical absorption bands.

SEM observations. Conventional preparation techniques consist of breaking or cutting the sample and removal of the LC by solvent to expose the polymer network. One of the glass plates was removed when the cell was at the liquid nitrogen temperature. Then the semi-free sample is immersed for 2 hours at room temperature in a cyanobiphenyl LC in isotropic phase (CB15 from Merck Ltd.). This intermediary step – before the immersion in a non-mesogenic isotropic solvent – facilitates the LC dissociation from the network (then it means that a LC in isotropic phase has to be dissolved in an isotropic solvent). Finally, the cell was immersed in cyclohexane for 3 days to leave bare the network. Samples were coated with a platinum film and observed using a Jeol JSM 6700F field-emission scanning electron microscope (SEM).

References

1. Small, D. M., Liquid crystals in living and dying systems *J. Colloid. Interf. Sci.* **58**, 581-602 (1977).
2. Neville, A. C., *Biology of Fibrous Composites: Development Beyond the Cell* (Cambridge University Press, 1993).

3. Bouligand, Y., Twisted fibrous arrangements in biological materials and cholesteric mesophases *Tissue Cell* **4**, 189-217 (1972).
4. Livolant, F. & Leforestier, A., Condensed phases of DNA: structures and phase transitions, *Prog. Polym. Sci.* **21**, 1115-1164 (1996).
5. Reis, D., Vian, B. & Roland, J.-C., Cellulose-glucuronoxylans and plant cell wall structure *Micron* **25**, 171-187 (1994).
6. Giraud-Guille, M.-M., Twisted plywood architecture of collagen fibrils in human compact bone osteons *Calcif. Tissue Int.* **42**, 167-180 (1988).
7. Yevdokimov, Yu. M., Skurdin, S. G., and Salyanov, V. I., The liquid-crystalline phases of double-stranded nucleic acids in vitro and in vivo, *Liq. Cryst.* **3**, 11, 1443-1459 (1988).
8. Van Winkle, D. H., Davidson, M. W., Chen, W. X. & Rill, R. L., Cholesteric helical pitch near persistence length DNA *Macromolecules* **23**, 4140-4148 (1990).
9. Dogic, Z. & Fraden, S., Cholesteric Phase in Virus Suspensions, *Langmuir* **16**, 7820-7824 (2000).
10. Sato, T., Nakamura, J., Teramoto, A. & Green, M. M., Cholesteric Pitch of Lyotropic Liquid Crystals *Macromolecules* **31**, 1398-1405 (1998).
11. Collings, P. J. & Hird, M. *Introduction to Liquid Crystals, Chemistry and Physics*, 223-243 (Taylor & Francis, London, 1997)
12. Bahadur, B. ed., *Liquid Crystals: Applications and Uses*, Vol. 1-3 (World Scientific, Singapore, 1990).
13. Srinivasarao, M., Nano-Optics in the Biological World : Beetles, Butterflies, Birds and Moths. *Chem. Rev.* **99**, 1935-1961 (1999).

14. Neville, A. C., Daily growth layers in animals and plants *Biol. Rev.* **42**, 421-441 (1967).
15. Neville, A. C. & Caveney, S., Scarabaeid beetle exocuticle as an optical analogue of cholesteric liquid crystals, *Biol. Rev.* **44**, 531-562 (1969).
16. Caveney, S., Cuticle reflectivity and optical activity in scarab beetles: the role of uric acid *Proc. Roy. Soc. Lond. B* **178**, 205-225 (1971).
17. de Gennes, P.-G. & Prost, J. *The Physics of Liquid Crystals*, 264-268 (Oxford University Press, 1993).
18. Kuball, H.-G. & Höfer, T., in *Chirality in Liquid Crystals* (eds Kitzerow, H.-S. & Bahr, C.) 86-88 (Springer-Verlag, New-York, 2001).
19. Huff, B. P., Krich, J. J. & Collings, P. J., Helix inversion in the chiral nematic and isotropic phases of a liquid crystal *Phys. Rev. E* **61**, 5, 5372-5378 (2000).
20. Slaney, A. J., Nishiyama, I., Styring, P. & Goodby, J. W., Twist Inversion in a Cholesteric Material containing a Single Chiral Centre *J. Mater. Chem.* **2**, 8, 805-810 (1992).
21. Styring, P., Vuijk, J. D., Slaney, A. J. & Goodby, J. W., Inversion of Chirality-dependent Properties in Optically Active Liquid Crystals *J. Mater. Chem.* **3**, 4, 399-405 (1993).
22. Stegemeyer, H., Siemensmeyer, K., Sucrow, W. & Appel, L., Liquid crystalline norcholesterylestere: influence of the axial methylgroups on the phase transitions and the cholesteric helix *Z. Naturforsch. A* **44A**, 11, 1127-1130 (1989).
23. Dierking, I. *et al.*, Investigations of the structure of a cholesteric phase with a temperature induced helix inversion and of the succeeding Sc* phase in thin liquid crystal cells *Liq. Cryst.* **13**, 1, 45-55 (1993).

24. Kuball, H.-G., Muller, T. & Weyland, H.-G., Induced Cholesteric Phases of Chiral Aminoanthraquinones, *Mol. Cryst. Liq. Cryst.* **215**, 271-278 (1992).
25. Kuball, H.-G., Muller, T., Bruning, H. & Schonhofer, A., Chiral induction by optically active aminoanthraquinones in nematic phases *Mol. Cryst. Liq. Cryst.* **261**, 845-856 (1995).
26. Dierking, I. *et al.*, The origin of the Helical Twist Inversion in Single Component Cholesteric Liquid Crystals *Z. Naturforsch* **49**, 1081-1086 (1994).
27. Dierking, I. *et al.*, New diastereomeric compound with cholesteric twist inversion *Liq. Cryst.* **18**, 443-449 (1995).
28. Broer, D. J. & Heynderickx, I., Three Dimensionally Ordered Polymer Networks with a Helicoidal Structure *Macromol.* **23**, 2474-2477 (1990).
29. Dierking, I., Kosbar, L. L., Afzali-Ardakani, A., Lowe, A. C. & Held, G. A., Network morphology of polymer stabilized liquid crystals *Appl. Phys. Lett.* **71**, 17, 2454-2456 (1997).
30. Bouligand, Y., Liquid Crystals and Their Analogs in Biological Systems *Solid State Physics* **14**, 259-294 (1978).
31. Besseau, L. & Bouligand, Y. The twisted collagen network of the box-fish scutes *Tissue & Cell* **30**, 2, 251-260 (1998).
32. Dierking, I., Kosbar, L. L., Afzali-Ardakani, A., Lowe, A. C. & Held, G. A., Two-stage switching behaviour of polymer stabilized cholesteric textures *J. Appl. Phys.* **81**, 7, 3007-3014 (1997).
33. Yang, D.-K., Chien L.-C. & Fung Y.K., in *Liquid Crystals in Complex Geometries* (eds Crawford, G. P. & Zumer, S.) 103-142 (Taylor & Francis, London, 1996).

34. Hikmet, R. A. M. From Liquid Crystalline Molecules to Anisotropic Gels *Mol. Cryst. Liq. Cryst.* **198**, 357-370 (1991).
35. Heppke, G., Löttsch, D. & Oestreicher, F. Esters of (S)-1,2-propanediol and (R,R)-2,3-butanediol — Chiral Compounds Inducing Cholesteric Phases with a Helix Inversion *Z. Naturforsch.* **42a**, 279-283 (1987).
36. Besseau, L. & Giraud-Guille, M.-M. Stabilization of Fluid Cholesteric Phases of Collagen to Ordered Gellated Matrices *J. Mol. Biol.* **251**, 197-202 (1995).

Acknowledgements

We acknowledge Dr. S. Rauch, Dr. D. Loetzsch, Prof. G. Heppke and Ms. M. Dzionara (from Stranski-Laboratorium für Physikalische und Theoretische Chemie in Technische Universität Berlin) who participated to the synthesis of the helicity-inversion chiral dopant DL6 and provided us with it. C. Bourgerette (from CEMES) participated to the material preparation for SEM-FEG investigations and, with S. Leblond du Plouy (from University Paul-Sabatier, Toulouse), helped us during the observations.

Competing financial interests

The authors declare that they have no competing financial interests.

Correspondence and requests for materials should be addressed to M. M. (mitov@cemes.fr).

SUPPLEMENTARY INFORMATION

NATURE OF POLARIZERS FOR SPECTROSCOPY

Home-made circular polarizers were used when investigations with polarized incident light were necessary. For such a purpose, blends of CLC BL094 and BL095 (from Merck Ltd.) were made. These compounds are enantiomers which selectively reflect light at 548 nm at room temperature. BL094 (BL095) is right- (left-) handed. A nematic (*i.e.* infinite-pitch cholesteric) structure is obtained when the compounds are blended in the same proportions (racemic mixture). We got circular polarizers with a tunable-wavelength reflection band and a helix either right- or left-handed by varying the relative concentration of one enantiomer with the other one. As a consequence, the polarizers are also reflectors: a left- (right-) handed helix gives rise to a right (left) circular polarizer. A 25 ± 5 μm thick cell was then filled with the blend corresponding to a pass-band superimposed with the investigated reflection band of the sample. Figure 1S shows examples of transmission spectra of left and right circular polarizers used when investigations with polarized light were made (in the case of Figure 2). The left (right) circular polarizer corresponds to a BL094 : BL095 wt.% ratio equal to 57 ± 1 : 43 ± 1 (43 ± 1 : 57 ± 1). In the case of data in Figure 1, due to the fact that the helical pitch of the blend slightly decreases as a consequence of the photoreaction (see text), the pass-band for the polarizers which are used for the characterization of optical properties before UV-curing was different, which means that the ratio has to be changed; here the (right) circular polarizer corresponds to a BL094 : BL095 wt.% ratio equal to 56 ± 1 : 44 ± 1 (44 ± 1 : 56 ± 1).

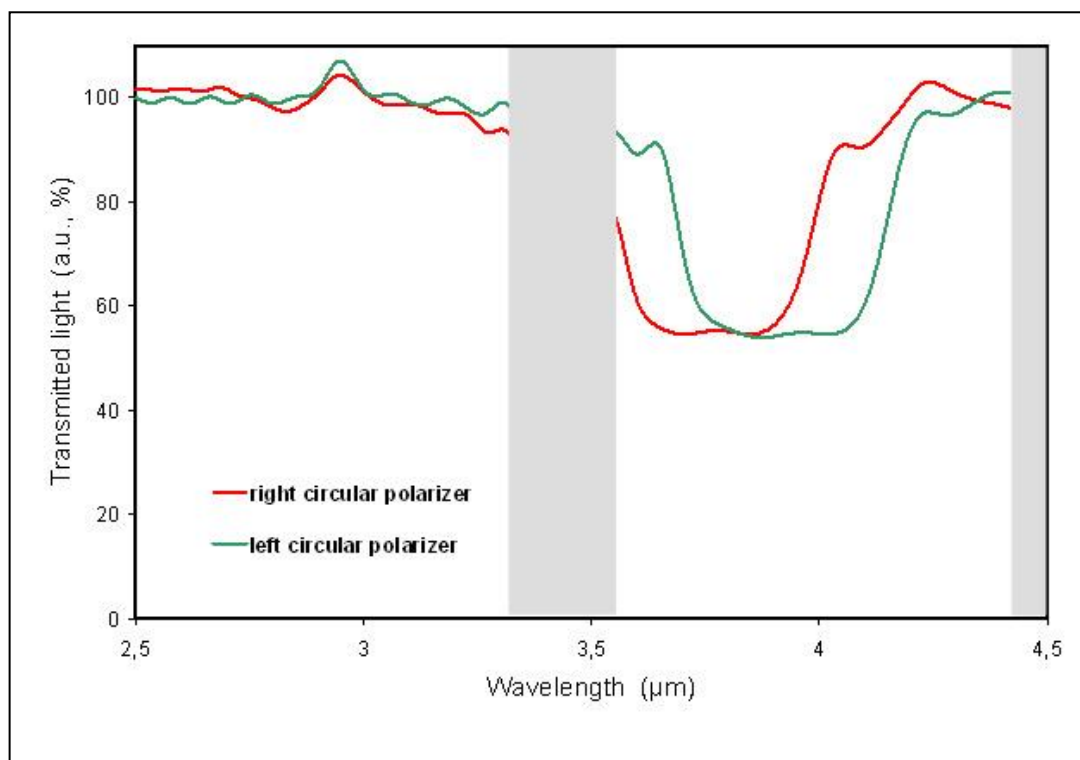


Figure 1S. Transmission spectra at room temperature of left and right circular polarizers when investigations with polarized light were made (in the case of Figure 2).